Near-Infrared Spectrometry as a Tool for Screening Meropenem for Quality

James T. Isaacs[1], Philip J. Almeter[1, 2], Aaron N. Hunter[1], Thomas A. Lyman[1], Stephanie P. Zapata[1], Bradley S. Henderson[1], Seth A. Larkin[1, 2], Eleonora Hasani[1], Uiyeol Yoon[1, 2], Adler Crumrin[1, 2], Jerod Smith[1, 2], Spencer Pergrem[1, 2], Ashton Plymale[1, 2], Bailee Ramnes[1, 2], Joshua D. Melson[1, 2], Jeffrey W. Reynolds[3], Eunice Relucio[2], Megan Bossle[2], Austin Lozier[2], Lindsey Long[2], Reagan Knight[2], Ryan W. Naseman[1, 2], Thomas L. Platt[1, 2], Robert A. Lodder[4,*]

University of Kentucky
Lexington, KY

1. Department of Pharmacy Services, University of Kentucky HealthCare, Lexington, KY 40536
2. Pharmacy Practice & Sciences, College of Pharmacy, University of Kentucky, Lexington, KY 40536
3. Department of Finance, University of Kentucky HealthCare, Lexington, KY
4. Department of Pharmaceutical Sciences, University of Kentucky, Lexington, KY 40536

*Author to whom correspondence should be addressed. Email: Lodder @ g.uky.edu
ORCID 0000-0001-6133-7561

RAPID COMMUNICATION

Abstract

Meropenem for Injection, USP is a sterile, pyrogen-free, white to pale yellow crystalline powder and is supplied in vials containing sufficient meropenem to deliver 1 g for intravenous administration.

The Drug Quality Task Force at the University of Kentucky has found variability in the near-infrared spectra of meropenem samples. The variability was found both within a lot (where one vial from six was 12.0 SDs from the other 5 vials) and between lots of the drug (where 8 vials were >3 SDs from the center of the library, and one of those was 6.1 SDs away from the center of the library). This variability was detected using a statistical analysis of the spectra that

included principal component analysis (PCA) and the BEST metric. Inter-lot variability was assessed using a spectral library of 90 meropenem vials obtained from 15 lots of drug from the same manufacturer. The results suggest that the drug may have been manufactured while the manufacturing process was operating outside of a state of process control.

Introduction

The University of Kentucky's (UK) Drug Quality Task Force (DQTF) was established in August of 2019 to engage in consumer-level quality assurance screening for drugs used within UK HealthCare's pharmacies (Isaacs, 2024a). The DQTF currently screens medications using Fourier transform near-infrared spectrometry (FTNIR) and Raman spectrometry for potential quality defects indicated by variability in absorbance peak intensities and locations. Through years of continuous monitoring, DQTF has assembled a spectral library containing medications typically used in a health system setting. Statistical analyses using the DQTF spectral library are performed to identify potential intra-lot and inter-lot variability in medications under review. Using Medwatch and publications in the scientific literature, the DQTF reports its findings in an effort to hold manufacturers accountable for GMP requirements and to improve patient outcomes by providing information on quality to augment the information on price that is already available. The increasing transparency is designed to improve the pharmaceutical supply chain.

Drug Product

Meropenem for Injection is a penem antibacterial indicated for the treatment of:

- Complicated skin and skin structure infections (adult patients and pediatric patients 3 months of age and older only).
- Complicated intra-abdominal infections (adult and pediatric patients).
- Bacterial meningitis (pediatric patients 3 months of age and older only).

To reduce the development of drug-resistant bacteria and maintain the effectiveness of Meropenem for Injection and other antibacterial drugs, Meropenem for Injection should only be used to treat or prevent infections that are proven or strongly suspected to be caused by susceptible bacteria (Drug Label Information, 1996). The drug is supplied as single dose clear glass vials of Meropenem for Injection, USP containing 1 gram (as the trihydrate blended with anhydrous sodium carbonate for re-constitution) of sterile meropenem powder.

The first lot screened was Fresenius Kabi lot 0002E01. After detecting an outlier (12.0 SDs) in lot 0002E01, a meropenem spectral library was formed from vial spectra in the DQTF database and lot 0002801 was compared to that database of spectra for all lots of meropenem from the same manufacturer. The lots in the library were 0001E11, 0002E01, 0002E11, 4A19L101, 4A20D01, 4A20D012, 4A20E07, 4A20E071, 4A20G01, 4A20G011, 4A20I21, 4A21C18, 4A21C22, 4A21D192, and 0018D91.

Figure 1 is a photo of the drug product from lot 0002E11. Meropenem for Injection, USP is a sterile, pyrogen-free, white to pale yellow crystalline powder and is supplied in vials containing sufficient meropenem to deliver 1 g for intravenous administration.

The 1 g/vial dose is supplied as 10 vials in a carton with NDC 55150-208-30. The dry powder should be stored at 20° to 25°C (68° to 77°F) [see USP Controlled Room Temperature].

The vial stoppers are not made with natural rubber latex.

Figure 1. Vials of meropenem drug product from lot 0002E11.

Background

Recent studies

Meropenem, a broad-spectrum carbapenem antibiotic, continues to be the subject of numerous recent scientific studies, both in clinical trials and in vitro experiments. Here's a summary of some key findings:

Clinical Trials:

- **Meropenem-vaborbactam (MV) for Carbapenem-Resistant Enterobacteriaceae (CRE) Infections:** Several studies have investigated the efficacy and safety of MV in treating CRE infections. A meta-analysis of clinical trials found that MV was associated with higher clinical cure rates and lower mortality compared to best available therapy (BAT) in patients with CRE infections (Zhou, 2023). Another study found that MV was effective in treating CRE infections in critically ill patients, with a clinical success rate of 65% and a survival rate of 90% (Tamma, 2020). However, some studies have reported the emergence of MV resistance, highlighting the need for continued surveillance and judicious use of this antibiotic (Shields, 2017).

In Vitro Experiments:

- **Meropenem Resistance Mechanisms:** In vitro studies have explored the mechanisms of meropenem resistance in various bacteria. One study found that the presence of carbapenemases, particularly KPC and NDM enzymes, is a major contributor to meropenem resistance in Enterobacteriaceae (Huang, 2022). Another study investigated the role of efflux pumps and porin mutations in conferring meropenem resistance in Pseudomonas aeruginosa (Li, 2019). These findings contribute to our understanding of resistance development and can inform strategies to combat it.

- **Combination Therapies:** In vitro experiments have also evaluated the potential of meropenem in combination with other antibiotics. A study demonstrated synergistic activity of meropenem with colistin against multidrug-resistant Acinetobacter baumannii (Petrosillo, 2013). Another study found that the combination of meropenem and amikacin was effective against carbapenem-resistant Klebsiella pneumoniae (Lee, 2018). These findings suggest that combination therapies may be a promising approach to enhance the efficacy of meropenem against resistant strains.

Recalls

While there is no specific information available about recent Eugia meropenem recalls, Eugia US LLC (formerly known as AuroMedics Pharma LLC) has been involved in several recent product recalls:

1. Polymyxin B for Injection: A voluntary nationwide recall was initiated due to the presence of particulate matter (Eugia, 2022).
2. Methocarbamol Injection: Eugia US LLC issued a voluntary nationwide recall of Methocarbamol Injection, USP 1000 mg/10 mL (100mg/mL) due to the presence of white particles in the vials (FDA, 2024).
3. AuroMedics Acyclovir Sodium: A recall was issued for this product lot number AC22006 of AuroMedics Acyclovir Sodium Injection 500 mg per 10 mL (50 mg/mL), 10 mL single dose vial from the U.S. market due to a product complaint of dark red, brown and black particulates inside the vial.(FDA, 2022).
4. Dexamethasone: Eugia US LLC recalled vials of Dexamethasone sodium phosphate injection USP 120mg/30mL (MDV) from the US market due to OOS (Out of specification results for commercial stability (California Board of Pharmacy, 2023).

Shortages

The recent shortages of Eugia meropenem can be attributed to several interconnected factors:

1. Manufacturing Issues: On February 5, 2024, Eugia announced a partial halt in production at its Unit-III facility in Hyderabad, India, affecting 56 national drug codes (NDCs), including meropenem (USP, 2024). This production halt was a direct result of observations made during an FDA investigation, highlighting significant compliance issues.
2. Regulatory Compliance Problems: The FDA issued a warning letter to Eugia Pharma Specialities Limited on August 15, 2024, detailing significant violations of Current Good Manufacturing Practice (CGMP) regulations (FDA Warning Letter, 2024). These violations included:
    - Issues with laboratory records
    - Problems with batch production and control records
    - Inadequate aseptic processing procedures
3. Supply Chain Disruptions: While not specific to Eugia, the global antibiotic supply chain is known to be fragile, with a limited number of manufacturers producing active pharmaceutical ingredients (APIs)(CIDRAP, 2018). Any disruption in this chain can lead to shortages, especially when combined with manufacturing issues.
4. Increased Demand: The global use of antibiotics has risen significantly in recent years, driven by rising living standards and increased healthcare access in low- and middle-income countries. This surge in demand can outpace production capabilities, particularly when manufacturing issues arise.

Methods

FTNIR (Fourier Transform Near-Infrared) Spectrometry

Using nondestructive analytical techniques, FTNIR spectra were collected from inventory as part of routine medication quality screening. A representative sample of individual vials were selected for screening and noted to be stored under the conditions required by the manufacturer in their original packaging. FTNIR spectra were collected noninvasively and nondestructively through the bottom of the vials using a Thermo Scientific Antaris II FTNIR Analyzer (Waltham, MA, USA)(Isaacs, 2024b).

Smoothing

Data smoothing is a technique used to remove noise from data. This can be done by fitting a smooth curve to the data, such as a cubic spline. Cubic splines are piecewise cubic polynomials that are continuous and have continuous first and second derivatives. This makes them very smooth and resistant to noise. Cubic splines can be easily fitted to data using least squares (Matlab, 2024)(Pollock, 1993).

Multiplicative Scatter Correction (MSC)

Multiplicative scatter correction (MSC) is a widely used spectrometric normalization technique. Its purpose is to correct spectra in such a way that they are as close as possible to a reference spectrum, generally the mean of the data set, by changing the scale and the offset of the spectra (Isaksson, 1988).

BEST (Bootstrap Error-Adjusted Single-sample Technique)

The BEST calculates distances in multidimensional, asymmetric, nonparametric central 68% confidence intervals in spectral hyperspace (roughly equivalent to standard deviations)(Dempsey, 1996). The BEST metric can be thought of as a "rubber yardstick" with a nail at the center (the mean). The stretch of the yardstick in one direction is therefore independent of the stretch in the other direction. This independence enables the BEST metric to describe odd shapes in spectral hyperspace (spectral point clusters that are not multivariate normal, such as the calibration spectra of many biological systems). BEST distances can be correlated to sample composition to produce a quantitative calibration, or simply used to identify similar regions in a spectral image. The BEST automatically detects samples and situations unlike any encountered in the original calibration, making it more accurate in chemical investigation than typical regression approaches to near-IR analysis. The BEST produces accurate distances even when the number of calibration samples is less than the number of wavelengths used in calibration, in contrast to other metrics that require matrix factorization. The BEST is much faster to calculate as well (O(n) instead of the $O(n^3)$ required by matrix factorization.)

Principal Components (PCs)

Principal component analysis is the process of computing the principal components of a dataset and using them to execute a change of basis (change of coordinate system) on the data, usually employing only the first few principal components and disregarding the rest (Joliffe, 2016). PCA is used in exploratory data analysis and in constructing predictive models. PCA is commonly utilized for dimensionality reduction by projecting each data point onto only the first few principal components to obtain lower-dimensional data while preserving as much of the original variation in the data as possible. The first principal component is the direction that maximizes the variance of the projected data. The second principal component is the direction of the largest variance orthogonal to the first principal component. Decomposition of the variance typically continues orthogonally in this manner until some residual variance criterion is met. Plots of PC scores help reveal underlying structure in data.

Subcluster Detection

In typical near-infrared multivariate statistical analyses, samples with similar spectra produce points that cluster in a certain region of spectral hyperspace. These clusters can vary significantly in shape and size due to variation in sample packings, particle-size distributions, component concentrations, and drift with time. These factors, when combined with discriminant analysis using simple distance metrics, produce a test in which a result that places a particular point inside a particular cluster does not necessarily mean that the point is actually a member of the cluster. Instead, the point may be a member of a new, slightly different cluster that overlaps the first. A new cluster can be created by factors like low-level contamination, moisture uptake, or instrumental drift. An extension added to part of the BEST, called FSOB (Fast Son of BEST) can be used to set nonparametric probability-density contours inside spectral clusters as well as outside (Isaacs, 2023)(Lodder, 1988), and when multiple points begin to appear in a certain region of cluster-hyperspace the perturbation of these density contours can be detected at an assigned significance level using r values, and visualized using quantile-quantile (QQ) plots. The detection of unusual samples both within and beyond 3 SDs of the center of the training set is possible with this method. Within the ordinary 3 SD limit, however, multiple instances are needed to detect unusual samples with statistical significance.

Artificial Intelligence Tools

Artificial intelligence (AI) tools, principally used for background information, include Gemini (Google LLC) and GPT-4 (OpenAI). AI can be used in a variety of ways, including to brainstorm, organize thoughts, develop arguments, and edit.

Results and Discussion

Intralot analysis

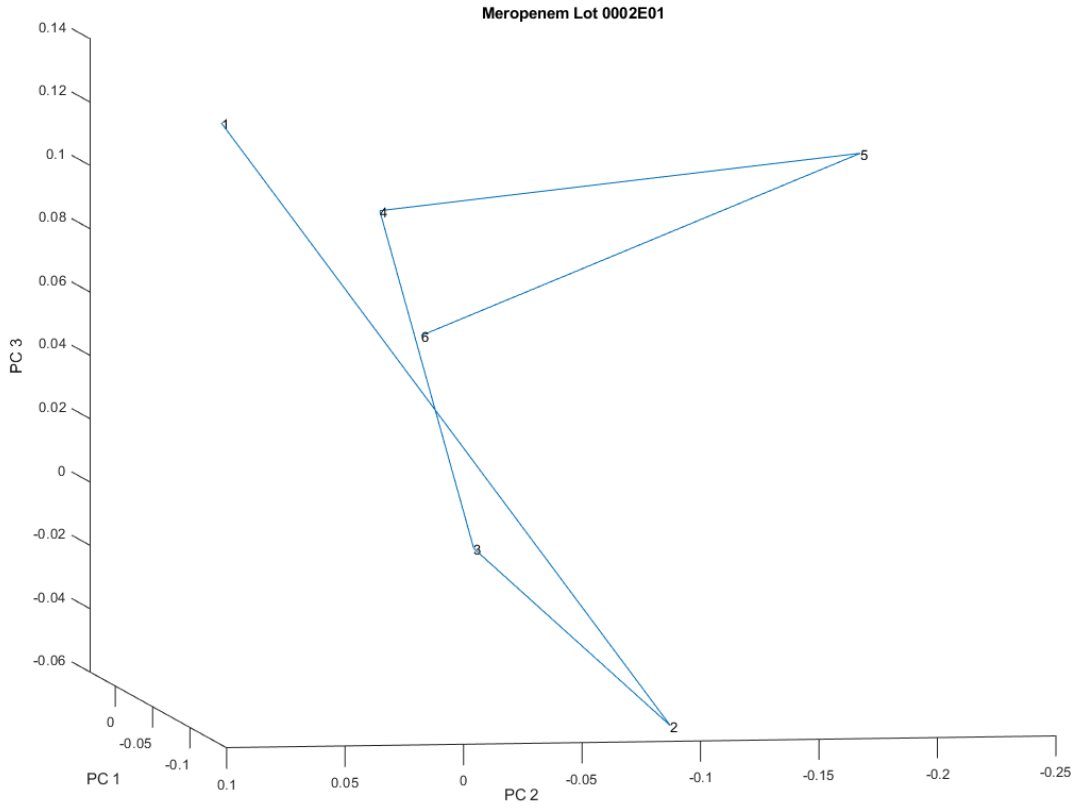

Figure 2. A principal component score plot of the first 3 PCs of meropenem lot 0002E01. Vial 5 is 12.0 SDs from the center of the cluster of the other vials.

Figure 2 displays the results of a PCA performed on samples from meropenem lot 0002E01. This specific plot uses the first three principal components (PC1, PC2, and PC3) as axes to represent the spectral data obtained from different vials within the same lot (intralot analysis). Vial 5 is significantly different from the other vials in the lot, positioned 12.0 standard deviations (SDs) away from the center of the cluster formed by the other vials. This significant deviation (12.0 SDs) for vial 5 suggests potential differences in its chemical properties compared to the other vials within the same lot. This variability might stem from issues during the manufacturing process, contamination, or degradation.

Interlot Analysis

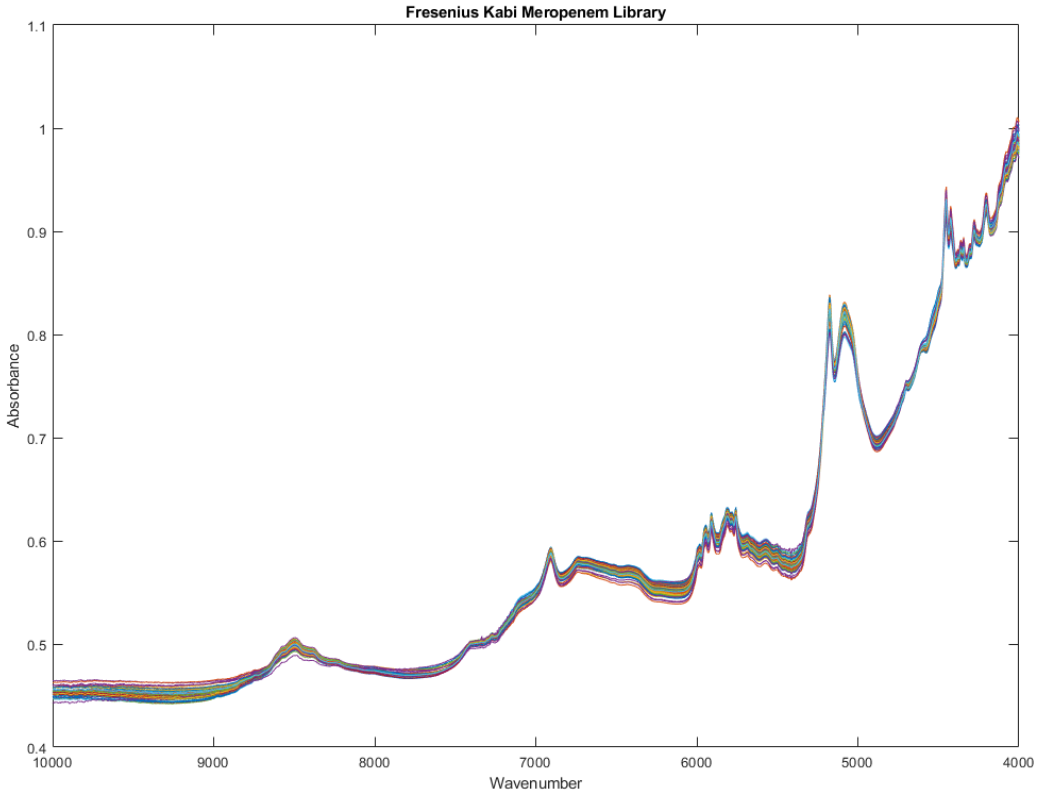

Figure 3. The FTNIR spectrum of each of the 90 vials in the spectral library from Fresenius Kabi meropenem.

Figure 3 depicts the overlaid FTNIR spectra for all 90 vials included in the spectral library created from the Fresenius Kabi meropenem vials. The x-axis represents the wavenumber (cm^{-1}), and the y-axis represents absorbance. Each line on the graph corresponds to the unique spectral signature of an individual vial. This spectral library, encompassing multiple lots, was assembled as part of the quality screening process to analyze variability across different vials and lots of the drug.

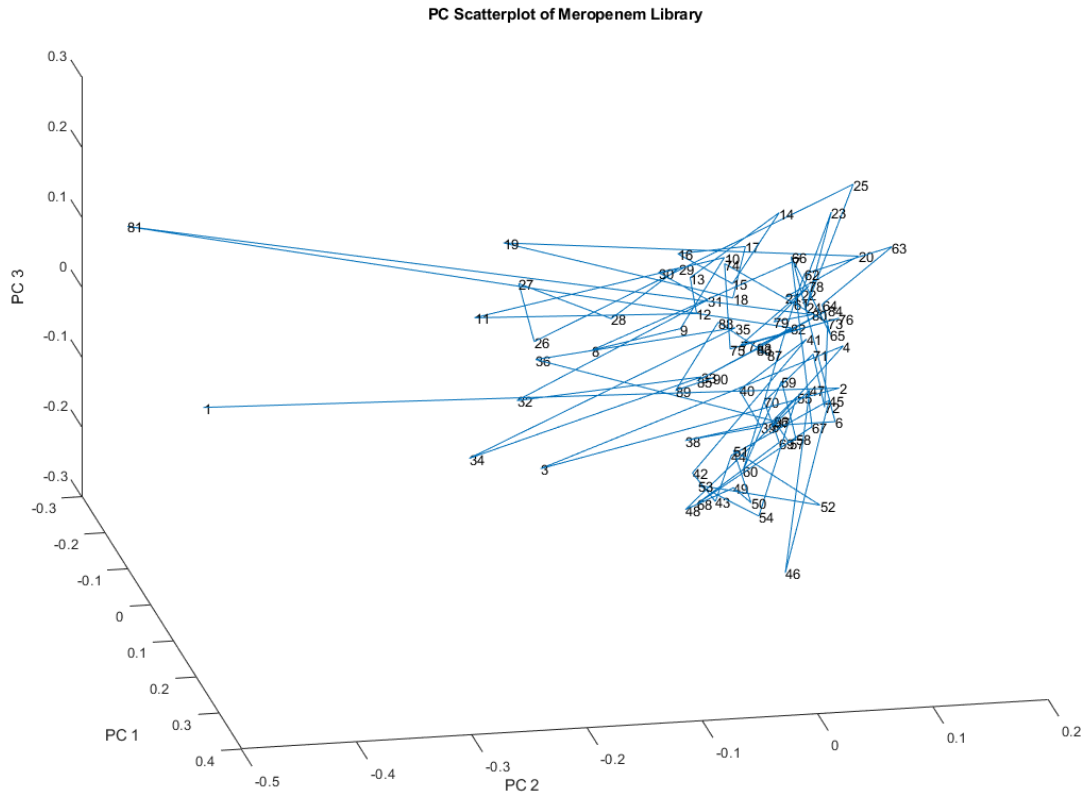

Figure 4. A principal component scatter plot using PC's 1, 2, and 3 to plot the data.

Figure 4 is a three-dimensional scatter plot that visualizes the data from the entire 90-vial meropenem spectral library using the first three principal components (PC1, PC2, and PC3) as axes. Each point in the plot represents an individual vial from the library. The plot helps to visualize the relationships and variability among the different vials based on their near-infrared spectra, as captured by the principal components.

The PC plot highlights outliers, which are points lying far away from the main cluster of data points. Eight vials were found to be more than 3 standard deviations (SDs) from the center of the library, with one vial (also identified as Vial 81 in Figure 5, which is a rotation of Figure 4) being 6.1 SDs away.

Principal Component Analysis (PCA) identifies the directions (principal components) in the data that capture the most variance. The first principal component (PC1) represents the direction of the largest variance, PC2 represents the next largest variance orthogonal to PC1, and so on.

If several outliers share a common underlying cause for their difference from the main group (e.g., a specific variation in manufacturing, moisture content, or degradation), this shared variation might be strongly represented by one or a combination of the first few principal

components. Consequently, these outliers would appear aligned along the direction(s) corresponding to those principal components in the scatter plot.

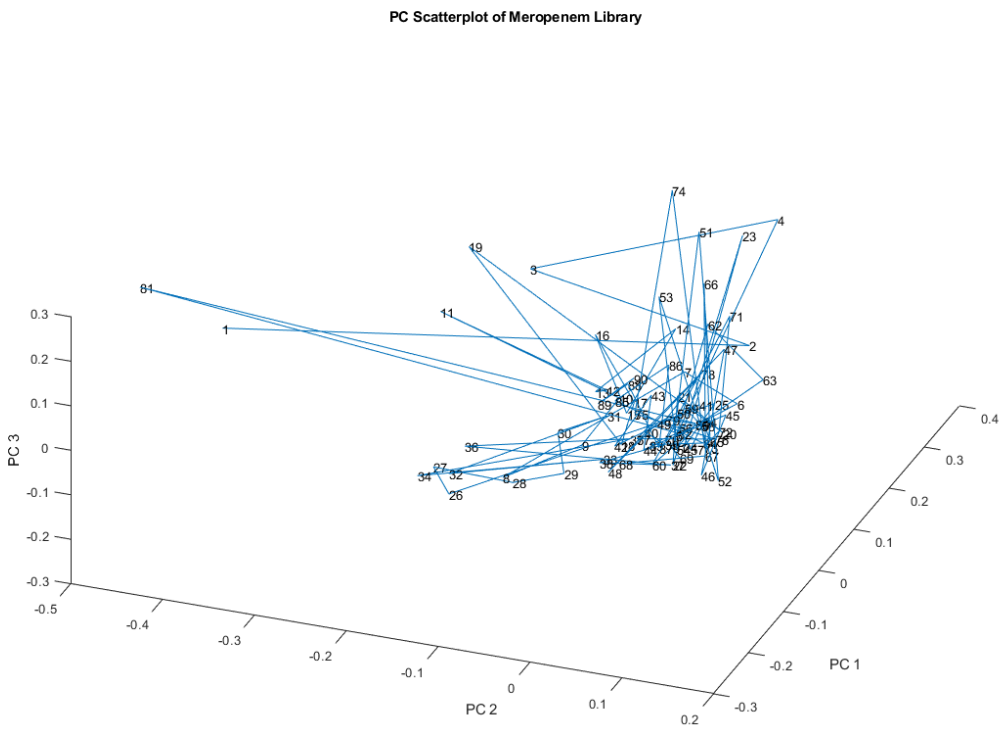

Figure 5. Another view (obtained by rotation of Figure 4) of a principal component scatter plot using PC's 1, 2, and 3 to plot the data. Vial 81 is 6.1 SDs from the center of the other vials.

Figure 5 is another rotation of Figure 4. It is important to have another view of the 3D scatter plot shown in Figure 4 because:

- *Revealing Hidden Structures:* Three-dimensional plots can be complex. Points can cluster together or hide behind one another depending on the viewing angle. Rotating the plot, as done to create Figure 5, provides a different perspective that can reveal structures, clusters, or individual points that were obscured in the original view.
- *Better Outlier Identification:* The rotated view in Figure 5 allows for a clearer visualization of the data distribution. This can make it easier to identify and examine specific points, such as outliers. The caption for Figure 5 specifically uses this view to point out that Vial 81 is 6.1 standard deviations away from the center of the cluster, which might have been less obvious or precisely located in the initial view presented in Figure 4.
- *Improved Spatial Understanding:* Seeing the data from multiple angles gives a better sense of the overall shape and spread of the data points in the three-dimensional space defined by the first three principal components. This aids in a more complete interpretation of the relationships revealed by the Principal Component Analysis (PCA).

In essence, providing Figure 5 as another view of Figure 4 helps ensure a more thorough and accurate understanding of the complex relationships within the meropenem spectral data library.

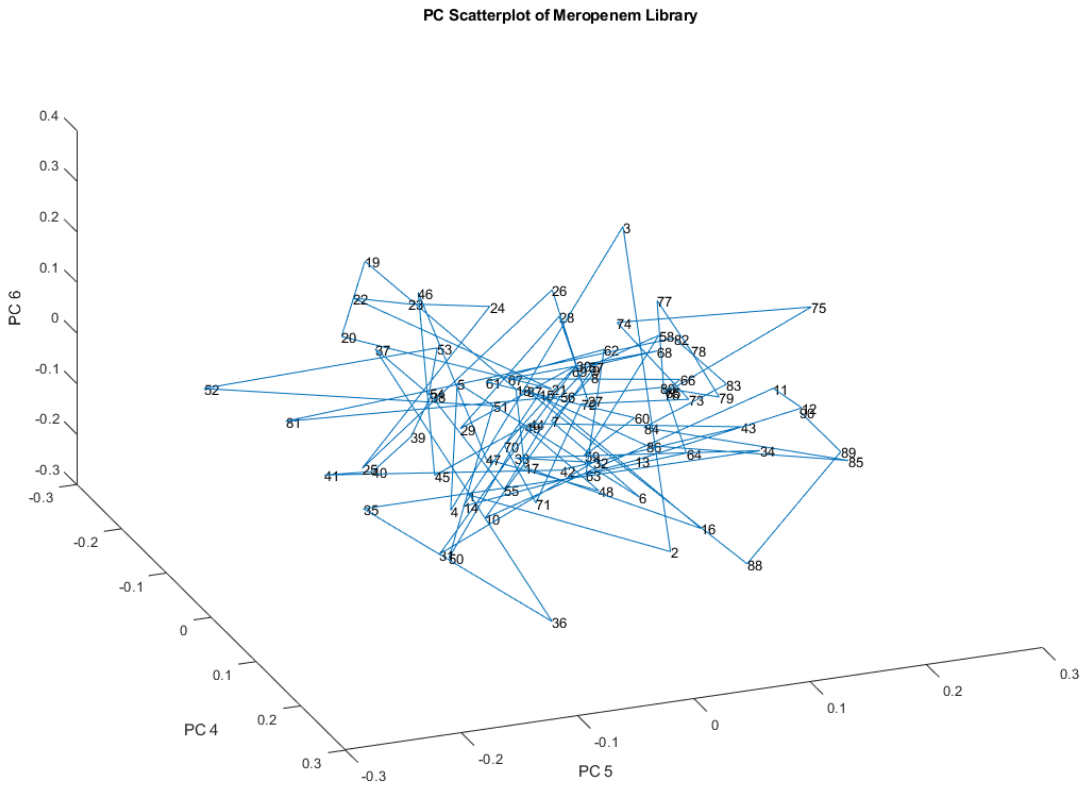

Figure 6. A principal component scatter plot using PC's 4, 5, and 6 to plot the data. No particular groups or outliers appear in the data.

Figure 6 plots the meropenem spectral library data using the 4th, 5th, and 6th principal components (PC4, PC5, and PC6). Principal Components (PCs) are derived in order of the amount of variance they explain in the data; PC1 explains the most, PC2 the next most, and so on. Therefore, PC4, PC5, and PC6 represent progressively smaller amounts of the total variation within the spectral data compared to PC1, PC2, and PC3 shown in Figures 4 and 5. Visually, the distribution of points in Figure 6 appears less structured than in the plots of the earlier PCs. There isn't a clear separation of distinct groups or obvious outliers standing far apart based on these components. This suggests that the main structural differences and the most significant variations distinguishing the vials (including the previously identified outliers) are primarily captured by the first three principal components. The variations represented by PC4, PC5, and PC6 are more subtle and contribute less to the overall differentiation between the samples. These later PCs might capture finer details or potentially incorporate more noise from the spectral measurements.

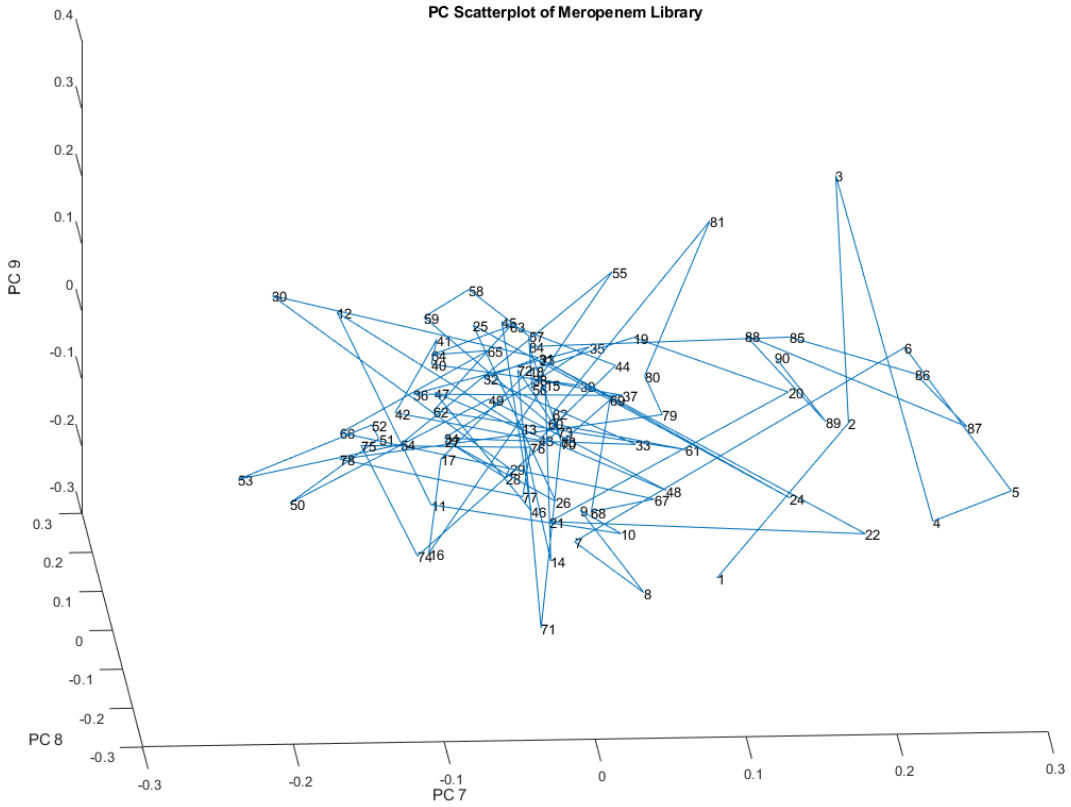

Figure 7. A principal component scatter plot using PC's 7, 8, and 9 to plot the data. A small subcluster appears to the right of the main cluster.

Figure 7 plots the meropenem spectral library data using the 7th, 8th, and 9th principal components (PC7, PC8, and PC9). These principal components capture even smaller amounts of the total variance in the spectral data compared to the earlier PCs (1-6) shown in previous figures. The plot shows a mostly scattered, seemingly random distribution of points. This indicates that PCs 7, 8, and 9 primarily represent very subtle variations or noise within the dataset, rather than major structural differences between the samples. Substantial noise is present by the ninth PC.

Regarding the small subcluster, methods exist to identify small groups of samples within a larger cluster that might indicate variations due to factors like minor contamination, moisture differences, or instrument drift. However, in Figure 7, plotting these high-order principal components (7, 8, and 9), does not clearly show a distinct, well-separated subcluster to the right of the main data cloud. The points in this region appear scattered in one direction rather than forming a coherent group based on these specific PCs.

The significant variability and outliers (e.g., Vial 5 being 12.0 SDs away from the center of its lot, or Vial 81 being 6.1 SDs away from the center of the library) were identified based on analyses involving the earlier, more dominant principal components and the BEST metric, which are sensitive to larger structural variations.

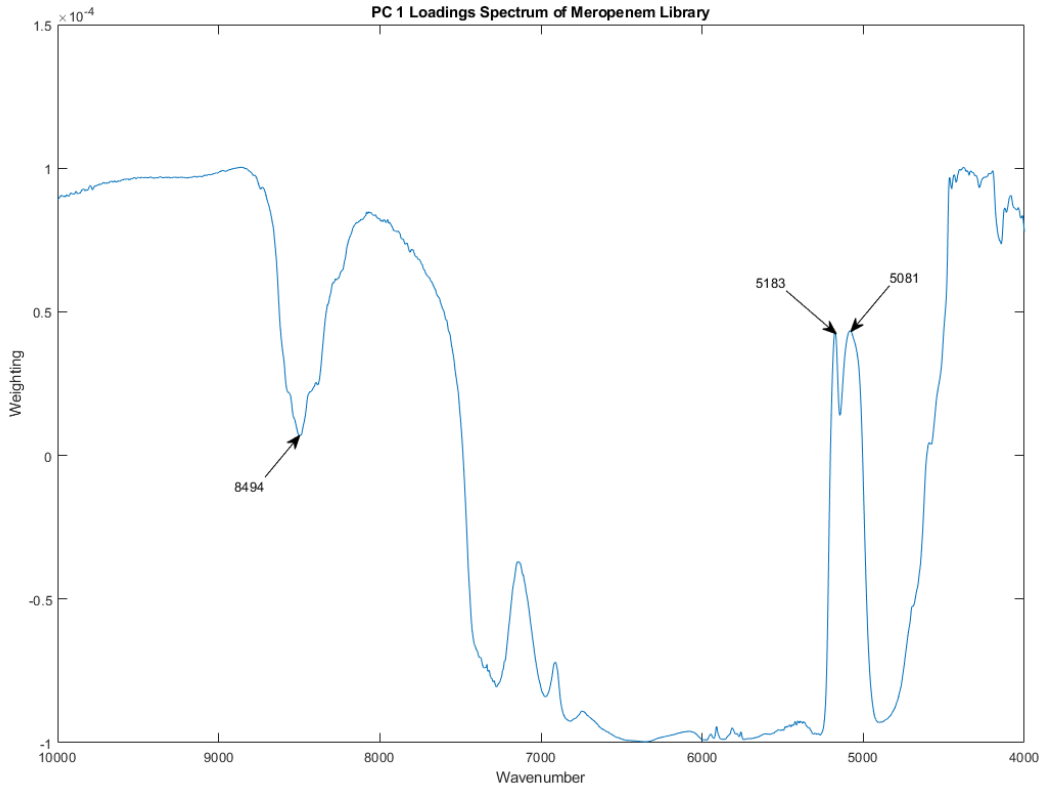

Figure 8. The principal component loadings spectrum for PC 1 of the meropenem library. Spectral features are noted at 5081, 5183, and 8494 cm^{-1}.

Figure 8 shows the principal component loadings spectrum for PC 1 of the meropenem library. Spectral features are noted at 5081, 5183, and 8494 cm^{-1}. This is important because it identifies specific spectral features related to the first principal component, which captures the largest variance in the data. These features can help pinpoint the chemical characteristics or differences contributing most significantly to the observed variations in the meropenem samples.

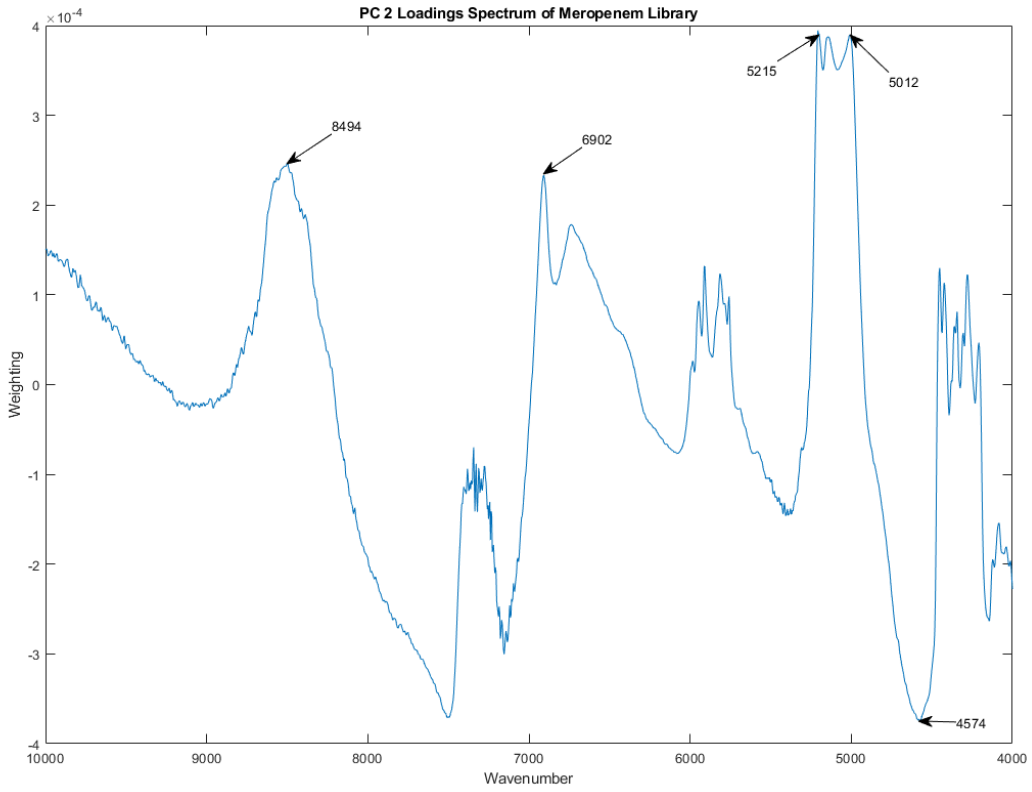

Figure 9. The principal component loadings spectrum for PC 2 of the meropenem library. Spectral features are noted at 4574, 5012, 5215, 6902, and 8494 cm^{-1}.

Figure 9 presents the principal component loadings spectrum for Principal Component 2 (PC 2) of the meropenem library. This visualization is important for understanding the spectral features that contribute most significantly to the variance captured in the second principal component of the pharmaceutical analysis. The spectrum highlights five significant spectral features at specific wavenumbers 4574 cm^{-1}, 5012 cm^{-1}, 5215 cm^{-1}, 6902 cm^{-1}, and 8494 cm^{-1}.

Each wavenumber region corresponds to specific molecular characteristics. The lower wavenumber region (4574-5215 cm^{-1}) is associated with combination bands and overtones of molecular vibrations. It indicates presence of C-H, O-H, or N-H functional groups and is iImportant for monitoring hydration states and structural integrity. The mid-range region (6902 cm^{-1}) represents higher-order overtones and combination bands useful for detecting manufacturing inconsistencies. Signals in this region can indicate structural variations in the compound. Signals in the high wavenumber region (8494 cm^{-1}) are typically related to C-H stretching overtones and can be associated with aromatic functional groups.

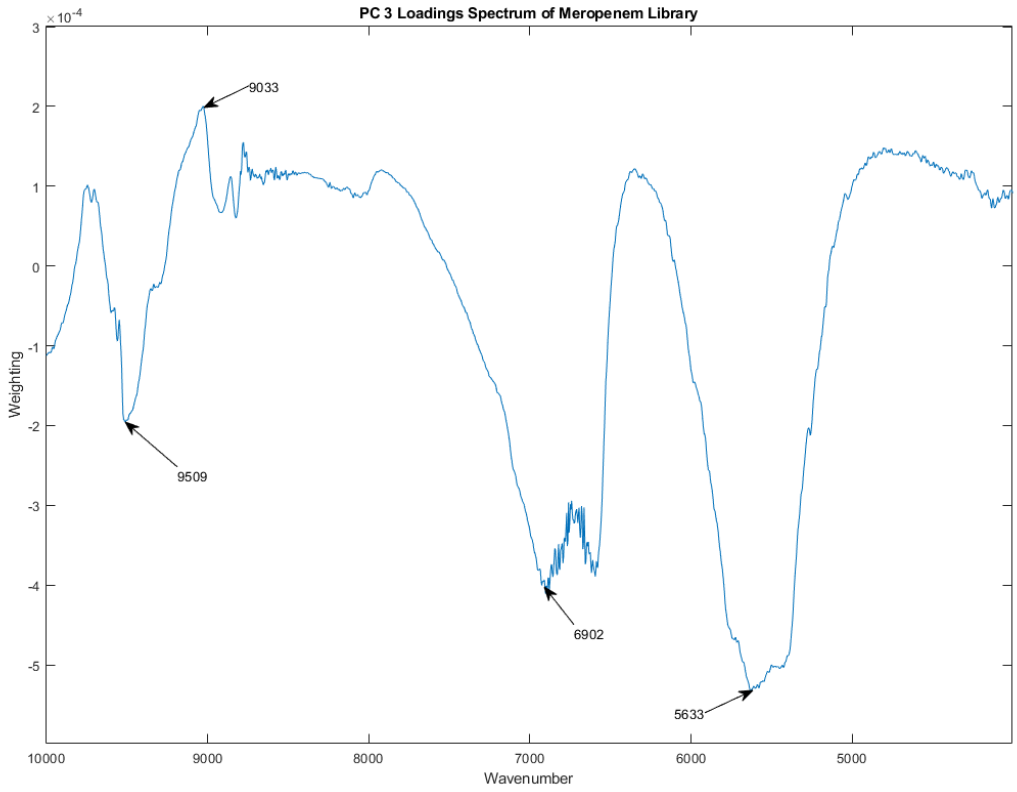

Figure 10. The principal component loadings spectrum for PC 3 of the meropenem library. Spectral features are noted at 5633, 6902, 9033, and 9509 cm^{-1}.

Figure 10 displays the loadings spectrum for the third principal component (PC3) calculated from the near-infrared (NIR) spectral library of the 90 meropenem vials. The loadings plot reveals the contribution or weighting of each original variable (in this case, each wavenumber in the NIR spectrum) to a specific principal component. Peaks (either positive or negative) in the loadings spectrum indicate wavenumbers where the spectral absorbance values have a significant influence on the score of a sample along the PC3 axis. In other words, these wavenumbers are important in defining the pattern of variation captured by PC3. The caption specifically highlights spectral features (wavenumbers with significant loadings) at 5633, 6902, 9033, and 9509 cm^{-1} for PC 3.

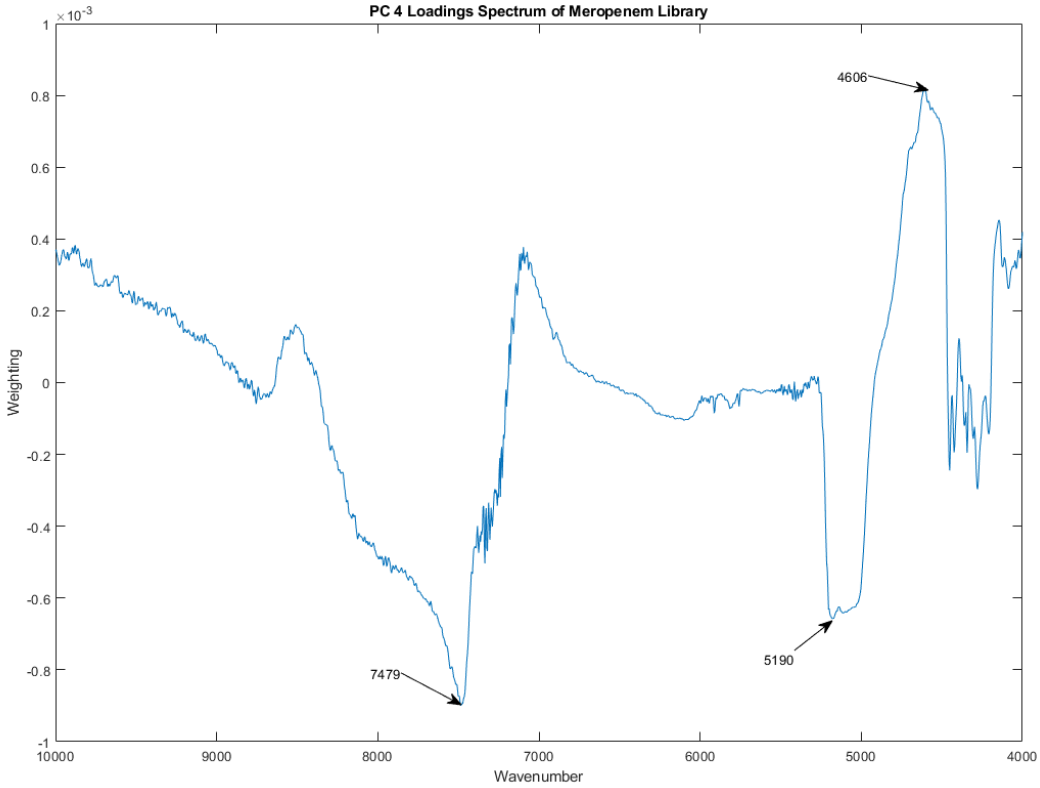

Figure 11. The principal component loadings spectrum for PC 4 of the meropenem library. Spectral features are noted at 4606, 5190, and 7479 cm^{-1}.

Figure 11 shows the loadings spectrum for the fourth principal component (PC4) calculated from the near-infrared (NIR) spectral library of the 90 meropenem vials. As mentioned previously when discussing loadings plots, this type of plot shows the contribution (weighting) of each original variable (each wavenumber in the NIR spectrum) to a specific principal component. Wavenumbers with high positive or negative loadings are significant contributors to the variation captured by PC 4. The caption specifically identifies spectral features (wavenumbers with significant loadings) at 4606, 5190, and 7479 cm^{-1} for PC 4.

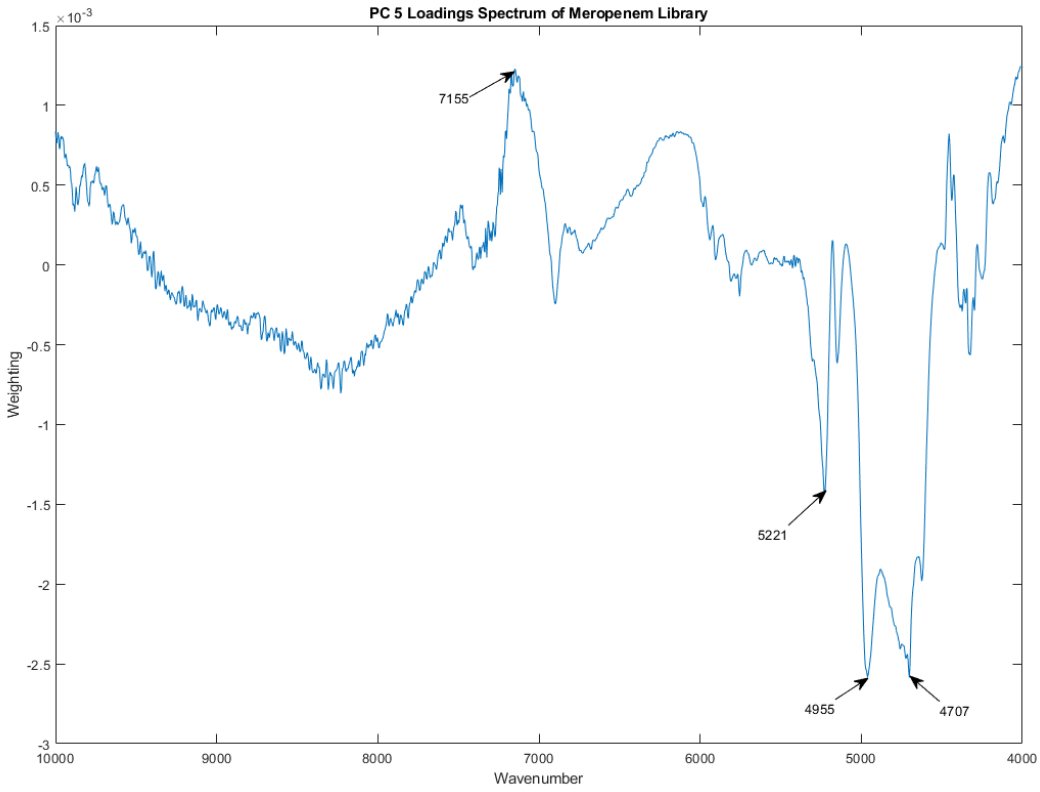

Figure 12. The principal component loadings spectrum for PC 5 of the meropenem library. Spectral features are noted at 4707, 4955, 5221, and 7155 cm^{-1}. Noise is beginning to creep in from the high wavenumber side of the spectrum.

Figure 12 shows the loadings spectrum for the fifth principal component (PC 5) calculated from the near-infrared (NIR) spectral library of the 90 meropenem vials. It displays the weighting (contribution) of each wavenumber to the variance captured by PC5. The caption highlights significant spectral features (wavenumbers with notable loadings) at 4707, 4955, 5221, and 7155 cm^{-1}.

This indicates that the variations represented by PC 5, particularly at the higher wavenumbers (shorter wavelengths, typically towards the left side of NIR spectra plots depending on convention, but here corresponding to the region > ~7500 cm^{-1}), are becoming increasingly influenced by random instrumental or measurement noise rather than solely reflecting systematic chemical or physical differences between the samples. The noise comes from the detector, which is less sensitive in this spectral region.

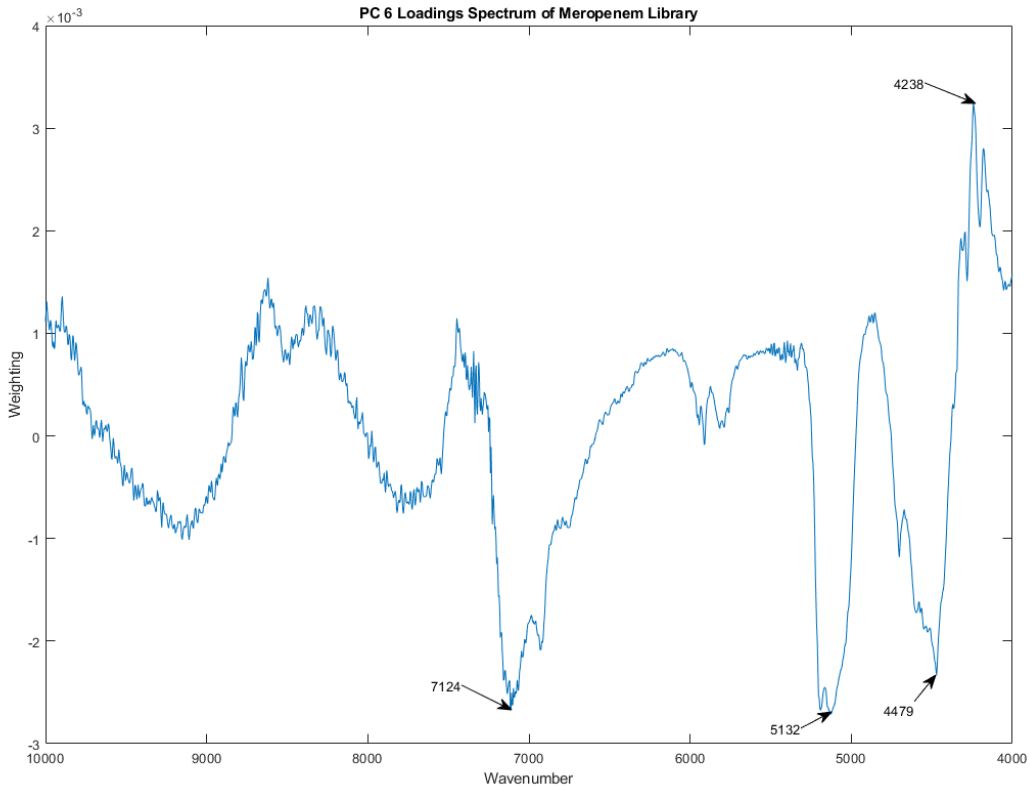

Figure 13. The principal component loadings spectrum for PC 6 of the meropenem library. Spectral features are noted at 4238, 4479, 5132, and 7124 cm^{-1}

Figure 13 displays the loadings spectrum for the sixth principal component (PC 6) calculated from the near-infrared (NIR) spectral library of the 90 meropenem vials in the spectral library. Similar to the other loadings plots discussed, it illustrates the contribution (weighting) of each original variable (each wavenumber in the NIR spectrum) to the specific pattern of variation captured by PC 6. Wavenumbers with high positive or negative loadings are significant contributors to the variance represented by PC 6. The caption specifically identifies spectral features (wavenumbers with significant loadings) at 4238, 4479, 5132, and 7124 cm^{-1} for PC 6.

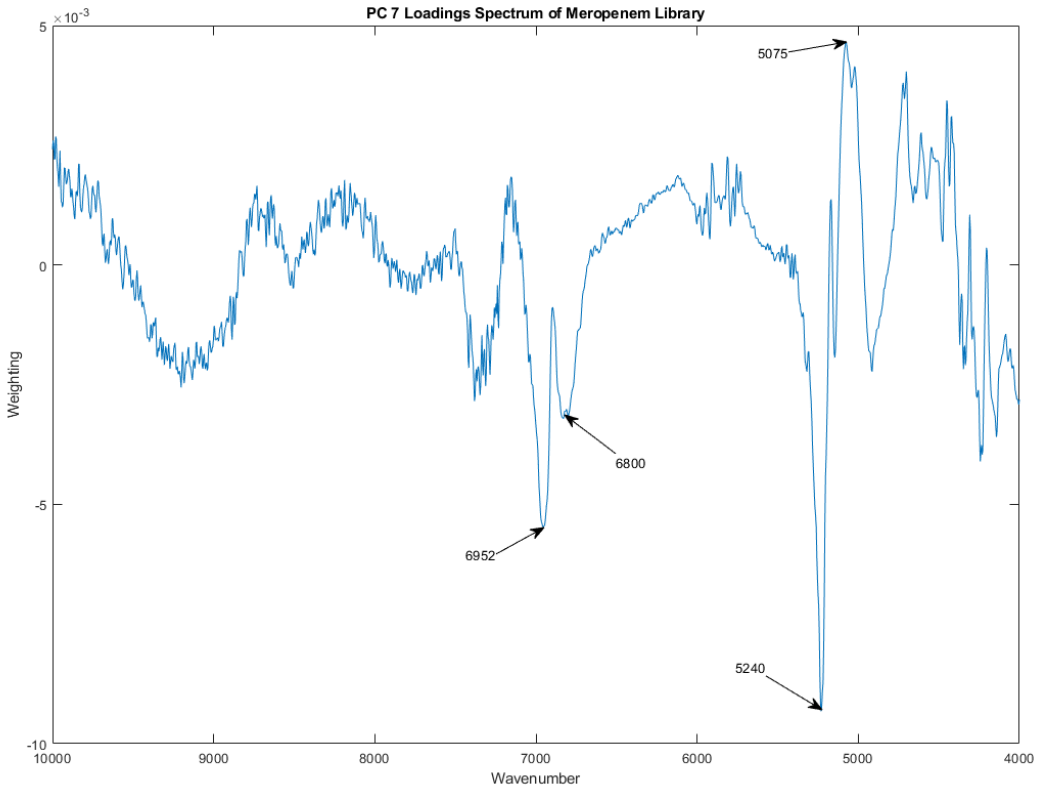

Figure 14. The principal component loadings spectrum for PC 7 of the meropenem library. Spectral features are noted at 5075, 5240, 6800, and 6952 cm^{-1}.

Figure 14 shows:the loadings spectrum for the seventh principal component (PC 7) calculated from the near-infrared (NIR) spectral library of the 90 meropenem vials. It shows the contribution (weighting) of each original variable (each wavenumber in the NIR spectrum) to the pattern of variation captured by PC 7. The y-axis represents the weighting, and the x-axis represents the wavenumber (cm^{-1}). Wavenumbers with high positive or negative loadings significantly influence a sample's score along the PC 7 axis. The caption specifically identifies spectral features (wavenumbers with significant loadings) at 5075, 5240, 6800, and 6952 cm^{-1} for PC 7. In summary, Figure 14 identifies the specific spectral regions (wavenumbers) most strongly associated with the seventh largest source of systematic variation detected within the meropenem spectral library data. Keep in mind that these higher-order PCs (like PC 7) typically represent smaller amounts of the total data variance compared to the initial PCs.

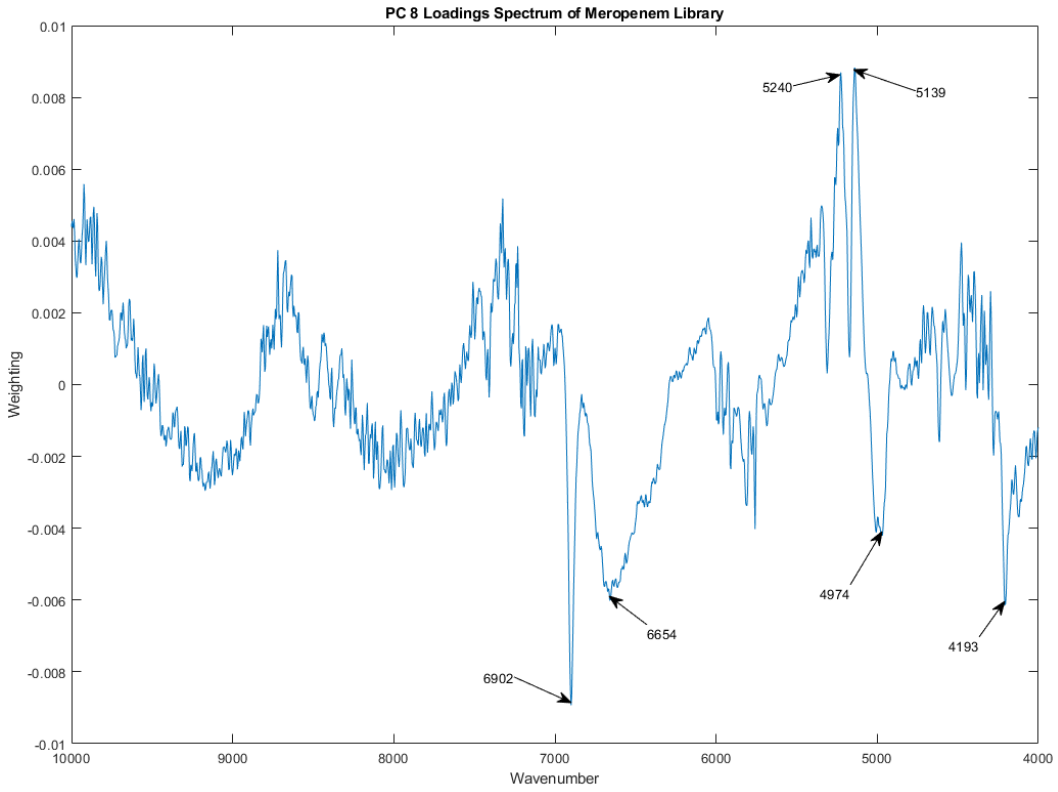

Figure 15. The principal component loadings spectrum for PC 8 of the meropenem library. Spectral features are noted at 4193, 4974, 5139, 5240, 6654, and 6902 cm^{-1}.

Figure 15 presents the principal component loadings spectrum for principal component 8 (PC 8) of the meropenem library. This visualization represents one of the higher-order principal components that captures subtle but potentially significant variations in the spectral data of meropenem samples.

Figure 15 presents the principal component loadings spectrum for Principal Component 8 (PC 8) of the meropenem library. This visualization represents one of the higher-order principal components that captures subtle but potentially significant variations in the spectral data of meropenem samples. The spectrum highlights six significant spectral features at specific wavenumbers of 4193 cm^{-1}, 4974 cm^{-1}, 5139 cm^{-1}, 5240 cm^{-1}, 6654 cm^{-1}, and 6902 cm^{-1}. The wavenumbers have chemical significance and each wavenumber region corresponds to specific molecular characteristics. The region around 4193 cm^{-1} is associated with overtone or combination bands of O-H, N-H, or C-H stretching vibrations, and often indicates presence of alcohols, amines, or hydrocarbons. The 4974-5240 cm^{-1} region is related to the second overtone of C-H stretching vibrations and thus is important for identifying and quantifying

hydrocarbons. It is also useful for detecting combination bands involving C-H, N-H, or O-H groups. The region around 6654-6902 cm^{-1} is associated with first overtone of O-H stretching vibrations and is crucial for monitoring moisture content and alcohol presence. It can also indicate higher overtones or combination bands of various molecular vibrations.

PC 8, as a higher-order component, captures subtle variations not evident in earlier principal components. The higher-order components help detect minor impurities, slight process deviations, and subtle chemical variations in the product. This ability in turn supports manufacturing process monitoring and enables detection of minor but potentially significant changes in process parameters, product composition, and manufacturing consistency.

Naturally, PC 8 has a connection to previous principal components. The PC 8 information complements the analysis shown in Figures 8-14 (PC 1-7). Also, some spectral features in Figure 15 overlap with earlier PCs, such as 5240 cm^{-1} (also in PC 7) and 6902 cm^{-1} (also in PCs 2 and 3)

Figures 8-15 represent an important part of the spectral analysis of meropenem, capturing subtle but potentially significant variations. The identified wavenumbers can provide valuable insights into specific molecular characteristics and potential variations in the pharmaceutical product, contributing to a comprehensive quality control system that ensures product consistency and safety.

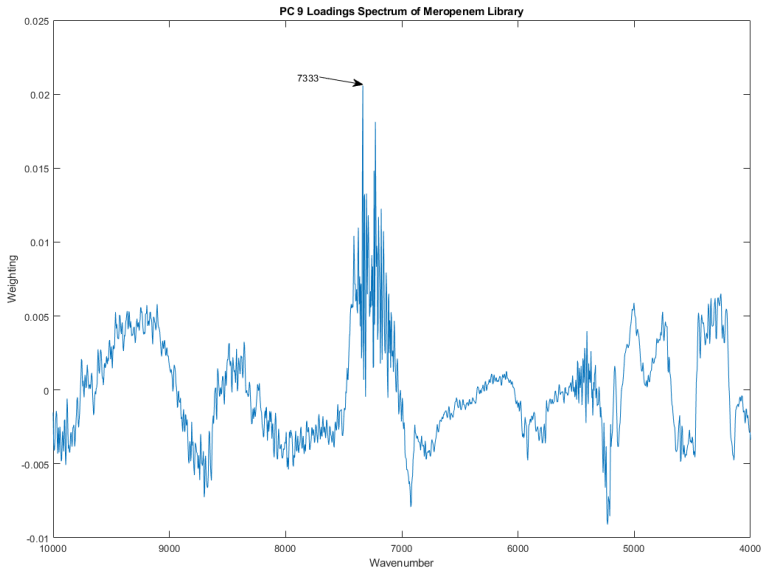

Figure 16. The principal component loadings spectrum for PC 9 of the meropenem library. A spectral feature is noted at 7333 cm^{-1}. Substantial noise is present by the ninth PC.

Figure 16 shows the loadings spectrum for the ninth principal component (PC9) calculated from the near-infrared (NIR) spectral library of the 90 meropenem vials. It illustrates the contribution (weighting) of each original variable (each wavenumber in the NIR spectrum) to the pattern of variation captured by PC9. The caption notes a spectral feature at 7333 cm^{-1}. The caption also explicitly states that "Substantial noise is present by the ninth PC". The dominant characteristic of this loadings plot, as noted in the text, is the significant presence of noise. This indicates that PC 9 captures very little systematic variance related to the chemical or physical properties of the samples and is primarily composed of random fluctuations from the measurement process.

Conclusion

A sample of 6 vials from the initially screened lot of drug contained one vial with a spectrum 12.0 multidimensional standard deviations away from the center of the cluster of vial spectra, suggesting that this vial's contents may have had different chemical properties compared to the others. This could be due to variability in the manufacturing process, contamination, or degradation of the drug. Factors that could contribute to variability in the pharmaceutical manufacturing process include:

- **Raw material variability:** The starting materials used to make the drug may have inconsistent quality or purity.
- **Equipment issues:** Malfunctions or inconsistencies in the equipment used during manufacturing can lead to variations in the final product.
- **Process parameters:** Fluctuations in temperature, pressure, or other process parameters can affect the chemical reactions involved in drug production.
- **Human error:** Mistakes by operators can introduce variability into the process.
- **Environmental factors:** Changes in humidity, temperature, or other environmental conditions within the manufacturing facility can impact the process.

As a result of this finding, the available spectral library of Fresenius Kabi meropenem (1 g/vial), consisting of 90 vials from 15 lots, was screened using FTNIR spectrometry and the BEST metric. Eight (8) vials were >3 SDs from the center of the library. Furthermore, one of those 8 vials was 6.1 SDs away from the center of the library. The variability observed in the NIR spectra of meropenem samples, both within and between lots, raises concerns about the consistency of the manufacturing process. The presence of a vial with a significantly different spectrum suggests potential inconsistencies in the drug's chemical properties, which could impact its safety and efficacy. These spectrometric results do not prove an excess level of impurities or adulteration. However, they suggest that the manufacturing process may have been operating outside of a state of process control. Additional investigation is needed.

Acknowledgements

The project described was supported in part by the National Center for Research Resources and the National Center for Advancing Translational Sciences, National Institutes of Health, through Grant UL1TR001998. The content is solely the responsibility of the authors and does not necessarily represent the official views of the NIH.

References

California Board of Pharmacy, (2023). Eugia US LLC (f/k/a AuroMedics Pharma LLC), https://www.pharmacy.ca.gov/about/recall_alerts/053024_eugia.pdf, retrieved Dec. 17, 2024.

CIDRAP, (2018). Report: Fragile supply chain causing antibiotic shortages, resistance threat, https://www.cidrap.umn.edu/antimicrobial-stewardship/report-fragile-supply-chain-causing-antibiotic-shortages-resistance, retrieved Dec. 18, 2024.

Dempsey, R. J., Davis, D. G., Buice Jr, R. G., & Lodder, R. A. (1996). Biological and medical applications of near-infrared spectrometry. Applied Spectroscopy, 50(2), 18A-34A.

Drug Label Information, (1996). https://dailymed.nlm.nih.gov/dailymed/drugInfo.cfm?setid=bf1d3433-9e3f-40a0-8bff-c8ceaa8bab7c#Section_1.1, retrieved Dec. 18, 2024

Eugia, (2022). Eugia US Issues Voluntary Nationwide Recall of Polymyxin B for Injection USP, 500,000 Unit per Vial, Due to the Presence of Particulate Matter, https://eugiaus.com/news/auromedics-pharma-llc-issues-voluntary-nationwide-recall-of-polymyxin-b-for-injection-usp-500000-unit-per-vial-due-to-the-presence-of-particulate-matter/, retrieved Dec. 17, 2024.

FDA, (2022). Eugia US LLC Issues Voluntary Nationwide Recall of Acyclovir Sodium Injection 500 mg per 10 mL (50 mg/mL), Due to the Presence of Particulate Matter, https://www.fda.gov/safety/recalls-market-withdrawals-safety-alerts/eugia-us-llc-issues-voluntary-nationwide-recall-acyclovir-sodium-injection-500-mg-10-ml-50-mgml-due, retrieved Dec. 17, 2024.

FDA, (2024). Eugia US LLC (f/k/a AuroMedics Pharma LLC) Issues Voluntary Nationwide Recall of Methocarbamol Injection, USP 1000 mg/10 mL (100mg/mL) (Single Dose Vial) Due to Presence of White Particles. https://www.fda.gov/safety/recalls-market-withdrawals-safety-alerts/eugia-us-llc-fka-auromedics-pharma-llc-issues-voluntary-nationwide-recall-methocarbamol-injection

FDA, (2024). WARNING LETTER: Eugia Pharma Specialities Limited, https://www.fda.gov/inspections-compliance-enforcement-and-criminal-investigations/warning-letters/eugia-pharma-specialities-limited-681905-08152024, retrieved Dec. 18, 2024.

Huang, T. W., et al. (2022). Carbapenemase-Producing Enterobacterales: Epidemiology, Detection, and Treatment Options. Expert Review of Anti-infective Therapy, 20(11), 1271-1285.

Isaacs, J. T., Almeter, P. J., Hunter, A. N., Lyman, T. A., Zapata, S. P., Henderson, B. S., ... & Lodder, R. A. (2024a). Application of Near-Infrared Spectroscopy for Screening of Chlorothiazide Sodium Vials. Contact in context, 10-6084. DOI: 10.6084/m9.figshare.25773429

Isaacs, J.T., Almeter , P.J., Hunter, A.N., Lyman, T.A. , Zapata, S.P., Henderson, B.S., Larkin, S.A., Long, L.M., Bossle, M.N., Bhaktawara, S.A., Warren, M.F., Lozier, A.M., Melson, J.D., Fraley, S.R., Relucio, E.H.L. Felix, M.A., Reynolds , J.W., Naseman, R.W., Platt, T.L., Lodder, R.A., (2024b) Lack of Content Uniformity in Azacitidine Vials, CIC Pharmaceutical Sciences, DOI: 10.6084/m9.figshare.26828245. NIHMSID:2021229

Isaacs, J.T., Almeter, P.J., Henderson, B.S., Hunter, A.N., Platt, T.L., & Lodder, R.A. (2023), Nonparametric Subcluster Detection in Large Hyperspaces, CIC Computational Sciences, 1-24. DOI:10.6084/m9.figshare.23877213

Isaksson, T., & Næs, T. (1988). The effect of multiplicative scatter correction (MSC) and linearity improvement in NIR spectroscopy. Applied Spectroscopy, 42(7), 1273-1284. https://doi.org/10.1366/0003702884429869

Jolliffe, I. T., & Cadima, J. (2016). Principal component analysis: a review and recent developments. Philosophical Transactions of the Royal Society A: Mathematical, Physical and Engineering Sciences, 374(2065), 20150202.

Lee, Y. J., et al. (2018). In Vitro Synergistic Activity of Meropenem and Amikacin against Carbapenem-Resistant Klebsiella pneumoniae. *Journal of Microbiology and Immunology*, 52(11), 768-774.

Li, X. Z., et al. (2019). Efflux Pump-Mediated Resistance to Meropenem in Pseudomonas aeruginosa. Frontiers in Microbiology, 10, 1797.

Lodder, R. A., & Hieftje, G. M. (1988). Detection of subpopulations in near-infrared reflectance analysis. Applied spectroscopy, 42(8), 1500-1512.

Matlab. Smoothing Splines. https://www.mathworks.com/help/curvefit/smoothing-splines.html. Retrieved August 28, 2024.

Petrosillo, N., et al. (2013). In Vitro Activity of Colistin and Meropenem Alone and in Combination against Multidrug-Resistant Acinetobacter baumannii. Journal of Antimicrobial Chemotherapy, 68(4), 812-817.

Pollock, D. S. G. (1993). Smoothing with cubic splines. https://www.physics.muni.cz/~jancely/NM/Texty/Numerika/CubicSmoothingSpline.pdf. Retrieved May 28, 2023.

Shields, R. K., et al. (2017). Emergence of Meropenem-Vaborbactam Resistance During Treatment of KPC-Producing Klebsiella pneumoniae Infections. Antimicrobial Agents and Chemotherapy, 61(12), e01411-17.

Tamma, P. D., et al. (2020). Early Experience With Meropenem-Vaborbactam for Treatment of Carbapenem-resistant Enterobacteriaceae Infections. Open Forum Infectious Diseases, 7(12), ofaa541.

USP. (2024). USP Medicine Supply Map Impact Analysis: Aurobindo partially halts production at Eugia's Unit-III, https://www.usp.org/news/aurobindo-partially-halts-production-at-eugias-unit-iii, retrieved Dec. 18, 2024

Zhou, X., et al. (2023). Systematic Review and Meta-Analysis of Clinical Efficacy and Safety of Meropenem-Vaborbactam versus Best-Available Therapy in Patients with Carbapenem-Resistant Enterobacteriaceae Infections. International Journal of Molecular Sciences, 24(17), 9574.